

RSC Advances



This is an *Accepted Manuscript*, which has been through the Royal Society of Chemistry peer review process and has been accepted for publication.

Accepted Manuscripts are published online shortly after acceptance, before technical editing, formatting and proof reading. Using this free service, authors can make their results available to the community, in citable form, before we publish the edited article. This *Accepted Manuscript* will be replaced by the edited, formatted and paginated article as soon as this is available.

You can find more information about *Accepted Manuscripts* in the [Information for Authors](#).

Please note that technical editing may introduce minor changes to the text and/or graphics, which may alter content. The journal's standard [Terms & Conditions](#) and the [Ethical guidelines](#) still apply. In no event shall the Royal Society of Chemistry be held responsible for any errors or omissions in this *Accepted Manuscript* or any consequences arising from the use of any information it contains.

Reinforcing effect on tribological behaviour of nanoparticles due to a bimodal grain size distribution

Nan Xu, Weimin Li, Ming Zhang, Gaiqing Zhao, and Xiaobo Wang*

State Key Laboratory of Solid Lubrication, Lanzhou Institute of Chemical Physics, Chinese Academy of Sciences, Lanzhou 730000, China

Abstract: In this study, two kinds of calcite calcium carbonate nanoparticle additives (CN), with grain size of ca. 30 nm and 80 nm respectively, were synthesized via the carbonation method. Then a series of additives were prepared through tuning the grain size distribution and the corresponding tribological performances were also carefully investigated. Compared with uniform size additives, the performances of additives with a bimodal grain size distribution were improved obviously and the application range was further extended. Meanwhile, it can be observed that CN with large grain size could improve the tribological behavior under high frequency condition, whereas the CN with small grain size determined the load bearing capacity. The corresponding lubrication mechanisms were also investigated according to characterization results of wear scar surface, such as the morphology, composition and microstructure. The results indicated that a continuous protective film was formed on the contact surface and the corresponding mechanical properties determined the final lubricity. The enhancement on the tribological performances can be attributed to the improved toughness of the protective film, due to the reinforcing effect of bimodal grain size distribution.

Keywords:

Nanoparticle additive, reinforcing effect, bimodal grain size distribution, toughness

1 Introduction

Nanostructured materials with inhomogeneous structure are of great interest for the development of advanced materials, such as photocatalytic,¹ plasmonic,² and mechanical^{3, 4} technologies. Meanwhile, it is also one of research hotspots in the tribology.⁵⁻¹⁶ One example of such materials is the nanoparticle additive, which can effectively improve the load bearing capacity, and reduce the friction and wear.⁷⁻¹⁵ Under mixed or boundary lubrication condition, the mechanism of protective film works in the friction process.^{11, 12, 17} Based on the physical or chemical interaction between the additive and contact surface, protective films are formed under certain external conditions. The microstructures (e.g. crystal structure and chemical composition) generally determine whether these materials possess lubricity.^{5, 6, 12, 18} Moreover, it was found that additives always possessed a short time lubricity outside the optimal application range.^{12, 16, 17} The service life of lubricant mainly depends on the toughness or anti-wear property of the protective film.^{5, 6} Therefore, the limitation for improving the tribological performance can be low toughness or poor anti-wear property. These can be overcome by employing inhomogeneous microstructure.^{3-6, 19}

In previous studies,^{3, 4, 19} nanocrystalline metals, with a bimodal crystalline grain size distribution, always provided a combination of high strength and tensile ductility, which result in tough nanostructured metals. In the tribology, the coatings,^{5, 6} composed of two or more heterogeneous constituents, also show concurrent strengthening and toughening due to the synergetic interaction and bimodal

mechanical property distribution. Therefore, this strategy is favor of the development of high tough nanostructured materials, which maybe provide effective condition for further reinforcing lubricity and prolonging the service life.

In our previous work, it was observed that the calcite calcium carbonate nanoparticles additive with different sizes displayed size-oriented adaptability towards the test condition.¹² That is, the nanoparticles with large size display best lubricity under the high frequency and the smaller show optimum performances under high load. For further reinforcing the performance, a series of bimodal-size additives were prepared in this work. The reinforcing effect of bimodal grain size distribution on the tribological performance and the corresponding mechanisms were investigated thoroughly according to the characterization results.

2 Experimental Section

2.1. Synthesis of lithium-calcium grease with compound additives

Two kinds of calcite calcium carbonate nanoparticles (CN) with different sizes and the lithium-calcium grease were synthesized, as detailed in our previous work¹². The average diameters of the synthesized nanoparticles were ca. 30nm and ca. 80nm, denoted as CN1 and CN2, respectively. In order to study the reinforcing effect, a series of additives, with the CN1/CN2 mass ratio of 5:0, 4:1, 2.5:2.5, 1:4 and 0:5, were prepared. Then, compound additives were added into base grease, mixed by mechanical stirring and ground for five times on the triple-roller mill.

2.2. Tribological tests

The tribological performances of grease plus synthesized CN additives were evaluated via an Optimol-SRV IV oscillating friction and wear tester. The test was conducted in a conventional reciprocating “ball-on-block” mode, with an oscillating upper ball (AISI E52100 steel, 10mm in diameter, HV 710-730) and a fixed lower disc (AISI E52100, ϕ 24mm \times 7.9mm, HV 710-730). The test conditions were mainly designed to investigate the performances under rigorous conditions. To evaluate the anti-wear property, MicroXAM 3D non-contact surface mapping profiler was employed to measure the wear volumes of the wear scars on the lower disc. Each test above was repeated three times to ensure the effectiveness of the results. The wear rates in the friction process were calculated using the equation $K=V/T$, where V is the wear volume (in μm^3), T is the corresponding sliding time (in min).

2.3. Characterization

The morphology and crystalline structure of CN were investigated via transmission electron microscopy (TEM, FEI TECNAI G2 TF20) and X-ray diffractometer (XRD, Riga Ku D/max-RB) equipped with Cu $K\alpha$ radiation ($\lambda=1.54056 \text{ \AA}$, 40 kV, 30 mA). The morphologies and, chemical and phase compositions of wear scar surface were characterized by Scanning electron microscopy (SEM, JSM-5600LV), X-ray photoelectron spectroscopy (XPS, PHI-5702), and Raman spectroscopy (RS, Reinshaw InVia). The Raman spectra were excited by the laser line having a wavelength of 514.5nm from an argon ion laser.

3 Results and discussion

3.1 Materials Characterization

Figure 1 showed the morphology and crystal information of CN prepared via the carbonation method. It could be observed that the average diameters of CN1 and CN2 are ca. 30 nm and ca. 80 nm, as shown in the parts a and b of figure 1. The corresponding RS spectra and XRD spectra of CN were used to identify the crystalline composition. Figure 1c showed the main Raman bands at 280.3, 710.3, 1085.9 and 1435 cm^{-1} , which are attributed to calcite.²¹ The position and relative intensity of all diffraction peaks in the XRD pattern (figure 1d) matched well with the calcite peaks (CaCO_3 , JCPDS 25-1033). Therefore, the main phase was calcite.

3.2 Tribological properties

In this paper, the tribological performances of additives with different grain size distributions were investigated under rigorous test conditions. Figure 2a-c presented the friction coefficient curves under constant load (500 N) and different frequency. Under low reciprocating frequency (10 Hz) the curves corresponding to uniform size nanoparticle (CN1 or CN2) displayed sharp fluctuation in the initial stage, a phenomenon known as seizure condition (figure 2a). It indicated that stable and continuous boundary protective film could not be formed promptly. Through tuning the CN1/CN2 mass ratio, the tribological performances were obviously improved and the additive with the ratio of 2.5:2.5 showed stable and low friction curve for the entire test time. Under medium frequency condition (25 Hz), it displayed similar trend as shown in figure 2b. For the high frequency condition, the additive with more CN2 content displayed better lubricity (figure 2c). Figure 2d displayed the friction curves

under higher load condition (600 N, 25 Hz). The friction curve corresponding to the ratio of 2.5:2.5 could recover to stable value after the short seizure at the initial test stage. For other additives, the reciprocation movements cannot move on due to poor lubrication. It could be concluded that the additive with the ratio of 2.5:2.5 displayed the optimal lubricity under high load and low to medium frequency. In our previous work,¹² the tribological performances of uniform size nanoparticle have been investigated. In comparison, the additives with bimodal grain size distribution displayed enhanced load bearing capacity (from 400 N to 600 N).

For further revealing the reinforcing effect of bimodal grain size distribution, the tribological performances under high frequency condition were investigated. As shown in figure 3a, the additive with the CN1/CN2 mass ratio of 1:4 displayed the optimal lubricity under 40 Hz and 400 N. The service life under higher frequency condition (55 Hz) was extended obviously compared with the CN2 (figure 3b), which exhibited optimal lubricity among the uniform size nanoparticle additives.¹²

The wear volume values were also measured to evaluate the anti-wear property. As shown in figure 4, the wear volume decreases at first and then increases with the decrease of CN1/CN2 mass ratio. Under high applied load the additive with the ratio 2.5:2.5 shows the best anti-wear property. While for the high frequency condition, the optimal anti-wear property can be obtained by controlling the ratio at 1:4. The wear volumes of the additives with moderate size distribution are reduced by > 95% in comparison with the uniform size nanoparticle additives. The result was consistent with the tribological results as shown in figure 2 and figure 3. Figure 5 shows the

SEM images of the wear scars lubricated with two kinds of additives. It can be observed that the wear scar lubricated with bimodal-size additive was smooth, while the surface lubricated by the uniform size additive showed the signs of grooves and gouging.

For revealing the lubricating mechanism, the back-scattered electron image (BSEI) and energy dispersive X-ray spectroscopy (EDS) were proposed to determine the formation of protective film as shown in figure 6. Figure 6a showed SEM/BSEI of a magnified area of wear scar in figure 5b. There existed dark and bright areas on the surface. Through the SEM/EDS analysis, elements calcium could be observed obviously in the dark area, while for the bright area, there are trace calcium content. Therefore, the dark area and bright area corresponded to the protective film and substrate of the lower disc, respectively. For further clarifying the chemical states of elements of the protective film, XPS analysis was used to characterize the wear scars. As shown in figure 7, the XPS spectra analyses of O and Ca were given. The high peak of O1s at 531.7 eV was identified as oxygen in carbonate,²² while the peaks at 530.2 eV and 529.8 eV were attributed to the oxygen in Fe₃O₄ and Fe₂O₃, respectively.^{23,24} Meanwhile, the main Ca2p peak appearing at 347.4 eV and 351.1 eV corresponded to Ca 2p_{3/2} and Ca 2p_{1/2} in calcium carbonate.²² In addition, the Raman spectroscopy was used to identify the corresponding crystal structure. As shown in figure 8, the main Raman bands at 279.5, 1085.2 and 1435.9 cm⁻¹ matched well the Raman spectra of calcite. Therefore, it could be concluded that the CN deposited and formed a continuous protective film on the contact surface, which still

kept the original crystal structure after crushed by the rubbing contact. Based on the same chemical and crystal compositions, the difference of tribological performance may be due to the different intrinsic mechanical properties of protective films, which depend on the grain size in this work.

According to the Hall-Petch effect, the hardness and yield stress of nanocrystalline materials will increase with decreasing the grain size.^{3, 20, 25} The fine grain will provide high strength, which is beneficial to the load bearing capacity. It has been demonstrated in our previous work.¹² The nanoparticles with the minimum size displayed optimal load bearing capacity due to the formation of high strength protective film. However, it also can be observed that the lowest strength nanoparticles (maximum size) showed sub-optimal load bearing capacity, which is inconsistent with the Hall-Petch effect. Meanwhile, it displayed better lubricity under high frequency condition (40 Hz and 400 N) in comparison with low frequency condition (25 Hz and 400 N). These results indicated that the strength of the protective film was not the only one of the important factors that influenced the tribological performances. As we known, tensile deformation of the protective film will occur under rigorous test condition. The lubrication failure is due to unstable tensile deformation, which can be overcome via improving the ductility of the protective film. Compared with fine grain, the coarse grain could accumulate larger number of dislocation to elevate the ductility. Therefore, the tribological performances of maximum size nanoparticles were improved. More importantly, the inhomogeneous microstructure induces strain hardening mechanisms that stabilize the

tensile deformation, leading to a high tensile ductility. The simultaneous high strength and ductility will further result in a notable gain in toughness.^{5, 25} Here, toughness is used to express the application range and PV value (P-pressure, V-velocity). In this study, it is achieved by the bimodal grain size distribution strategy, which will have application in the development of high performance nanoparticle additives with notable toughness and wear resistance. As shown in figure 9, the wear volume and wear rate at different test stages were given for further clarifying the lubricating mechanism. As we know, friction is one process of wearing and continuous repairing and the anti-wear property could reflect the toughness of protective film. It can be observed that the wear volumes of appropriate additives always maintain at low level for the entire test time. Inadequate lubrication always results in serious wear from the initial stage. However, the wear rates of all additives decrease with time. It is suggested that all the additives have the effectively lubricating performance, but the toughness will determine the relative speed of wearing and repairing. For the high toughness protective film, the repairing speed takes a dominant position in the friction process. Therefore, the appropriate compound additives could form high tough protective film and display excellent performance under rigorous test condition. On the contrary, serious abrasion will happen. In addition, it can be observed that under high frequency condition, the compound additive with mass ratio of 1:4 shows the minimum wear volume value. Whereas the mass ratio of 2.5:2.5 corresponds to the optimal performance for the high load condition. Therefore, the toughness requirements under different test condition are different and can be reinforced via

tuning the grain size distribution. The hardness always plays more important role in high load condition and the ductility will favor to improve the tribological performance under the high frequency condition.

4. Conclusions

In summary, a series of additives with the CN1/CN2 mass ratio at 5:0, 4:1, 2.5:2.5, 1:4 and 0:5 were prepared. The tribological properties were obviously improved via tuning the size distribution. It can be observed that the load bearing capacity was increased from 400 N to 600 N and the service life under high frequency condition was obviously increased, compared with the uniform size CN additives. Meanwhile, the corresponding wear volumes are reduced by > 95%. The characterization results indicated that the lubricating mechanism of protective film works in this study. Based on the same chemical and crystal compositions, the final tribological performance was mainly determined by the toughness of the protective film. The additives, with a bimodal grain size distribution, provide a combination of high strength and tensile ductility, which further results in high toughness. Meanwhile, the hardness plays more important role in high load condition and the ductility favors the high frequency condition. In addition, the bimodal grains size distribution strategy gives excellent possibilities to design wear-resistance, friction and toughness. There is every reason to believe that the method suggested here is applicable to a wide class of materials.

Corresponding author

E-mail: wangxb@licp.cas.cn

Acknowledgment: This work was funded by the National 973 Program of China (Grant No. 2011CB706602) and the National Natural Science Foundation of China (Grant No. 51205384).

References

- 1 A. Kubacka, M. Fernandez-Garcia and G. Colon, *Chem. Rev.*, 2012, **112**, 1555.
- 2 M. Grzelczak, J. Pérez-Juste, P. Mulvaney and L. M. Liz-Marzán, *Chem. Soc. Rev.*, 2008, **37**, 1783.
- 3 Y. M. Wang, M. W. Chen, F. H. Zhou and E. Ma, *Nature*, 2002, **419**, 912.
- 4 Y. H. Zhao, T. Topping, J. F. Bingert, J. J. Thornton, A. M. Dangelewicz, Y. Li, W. Liu, Y. T. Zhu, Y. Z. Zhou and E. J. Lavernia, *Adv. Mater.*, 2008, **20**, 3028.
- 5 O. Wilhelmsson, M. Rålander, M. Carlsson, E. Lewin, B. Sanyal, U. Wiklund, O. Eriksson and U. Jansson, *Adv. Funct. Mater.*, 2007, **17**, 1611.
- 6 A. A. Voevodin and J. S. Zabinski, *Compos. Sci. Technol.*, 2005, **65**, 741.
- 7 A. H. Battez, R. Gonzalez, J. L. Viesca, J. E. Fernández, J. M. Díaz Fernández, A. Machadoc, R. Choud and J. Ribae, *Wear*, 2008, **265**, 422.
- 8 J. F. Zhou, Z. S. Wu, Z. J. Zhang, W. M. Liu and H. X. Dang, *Wear*, 2001, **249**, 333.
- 9 Z. S. Hu, R. Lai, F. Lou, L. G. Wang, Z. L. Chen, G. X. Chen and J. X. Dong, *Wear*, 2002, **252**, 370.
- 10 M. Akbulut, N. Belman, Y. Golan and J. Israelachvili, *Adv. Mater.*, 2006, **18**, 2589.
- 11 L. Rapoport, O. Nepomnyashchy, I. Lapsker, A. Verdyan, A. Moshkovich, Y. Feldman and R. Tenne, *Wear*, 2005, **259**, 703.

- 12 N. Xu, M. Zhang, W. M. Li, G. Q. Zhao, X. B. Wang and W. M. Liu, *Wear*, 2013, **307**, 35.
- 13 S. Chen and W. M. Liu, *Mater. Chem. Phys.*, 2006, **98**, 183.
- 14 V. Eswaraiyah, V. Sankaranarayanan and S. Ramaprabhu, *ACS Appl. Mater. Inter.*, 2011, **3**, 4221.
- 15 V. Khare, M. Q. Pham, N. Kumari, H. S. Yoon, C. S. Kim, J. I. Park and S. H. Ahn, *ACS Appl. Mater. Inter.*, 2013, **5**, 4063.
- 16 J. F. Ou, Y. Wang, J. Q. Wang, S. Liu, Z. P. Li and S. R. Yang, *J. Phys. Chem. C*, 2011, **115**, 10080.
- 17 M. R. Cai, Y. M. Liang, F. Zhou and W. M. Liu, *ACS Appl. Mater. Inter.*, 2011, **3**, 4580.
- 18 K. J. Sankaran, N. Kumar, J. J. Kurian, R. Ramadoss, H. C. Chen, S. Dash, A. K. Tyagi, C. Y. Lee, N. H. Tai and I. N. Lin, *ACS Appl. Mater. Inter.*, 2013, **5**, 3614.
- 19 C. J. Youngdahl, J. R. Weertman, R. C. Hugo and H. H. Kung, *Scripta Mater.*, 2001, **44**, 1475.
- 20 C. S. Pande and K. P. Cooper, *Prog. Mater. Sci.*, 2009, **54**, 689.
- 21 C. G. Kontoyannis and N. V. Vagenas, *Analyst*, 2000, **125**, 251.
- 22 M. I. Sosulnikov and Y. A. Teterin, *Doklady Akademii Nauk SSSR*, 1991, **317**, 418.
- 23 G. C. Allen and K. R. Hallam, *Appl. Sur. Sci.*, 1996, **93**, 25.
- 24 B. J. Tan, J. Kenneth, K. J. Klabunde and P. M. A. Sherwood, *Chem. Mater.*, 1990, **2**, 186.
- 25 Y. M. Wang and E. Ma, *Acta Mater.*, 2004, **52**, 1699.

Figure captions

Figure 1. TEM images of (a) CN1 and (b) CN2, and the corresponding Raman spectra (c) and XRD pattern (d) of CN1.

Figure 2. Friction coefficient of grease plus 5 wt.% CN additive with different CN1/CN2 mass ratio at (a) 500 N, 10 Hz; (b) 500 N, 25 Hz; (c) 500 N, 40 Hz; (d) 600 N, 25 Hz.

Figure 3. Friction coefficient of grease plus 5 wt.% CN additive with different CN1/CN2 mass ratio at (a) 400 N, 40 Hz; (b) 400 N, 55 Hz.

Figure 4. Wear volume of the lower disc lubricated by grease plus 5 wt.% CN additive with different CN1/CN2 mass ratio under rigorous condition (500 N, 25 Hz; 400 N, 40 Hz).

Figure 5. SEM images of wear scars lubricated by grease plus 5 wt.% CN additive with CN1/CN2 mass ratio of (a, c) 5:0 and (b, d) 1:4 under 400 N and 40 Hz.

Figure 6. SEM/BSEI (a) and SEM/EDS (b) of wear scar lubricated by grease plus 5 wt.% CN additive with CN1/CN2 mass ratio of 1:4 under 400 N and 40 Hz.

Figure 7. XPS spectra of wear scar lubricated by grease plus 5 wt.% CN additive with CN1/CN2 mass ratio of 1:4 under 400 N and 40 Hz.

Figure 8. Raman spectra of wear scar lubricated by grease plus 5 wt.% CN additive with CN1/CN2 mass ratio of 1:4 under 400 N and 40 Hz.

Figure 9. Wear volume and wear rate of wear scars lubricated by grease plus 5 wt.% CN additives under 400 N and 40 Hz with different CN1/CN2 mass ratio of (5:0; 1:4; 0:5).

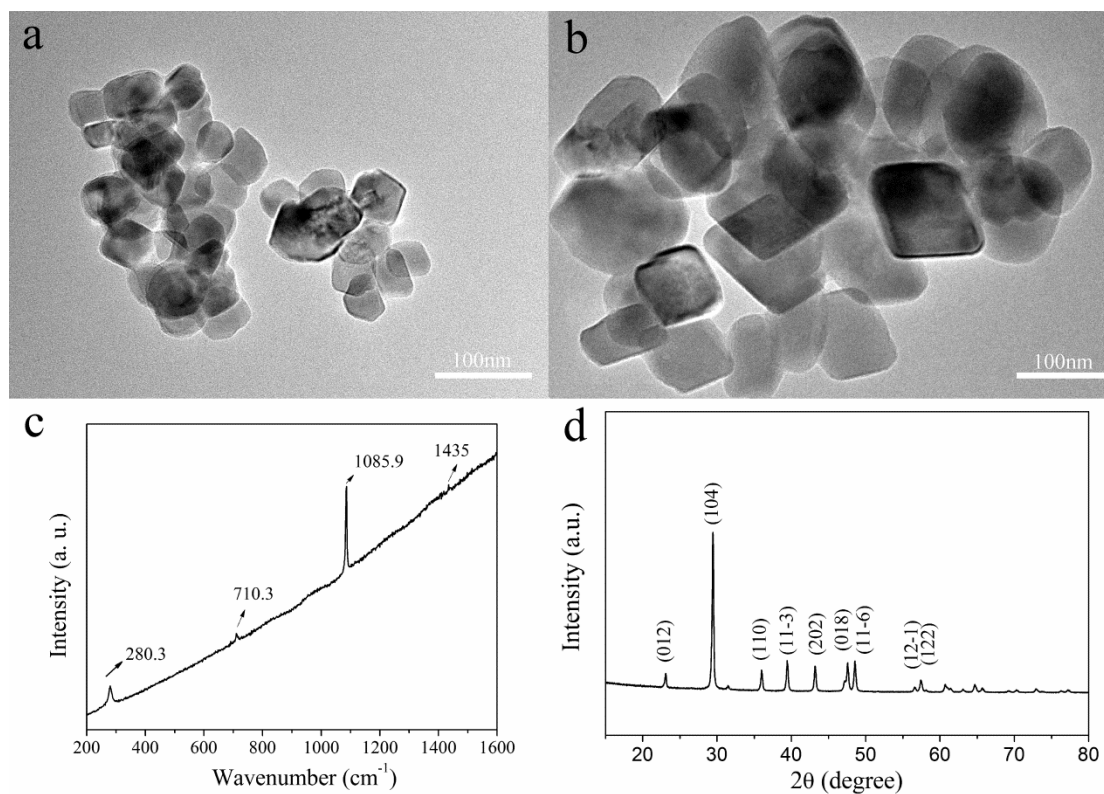


Figure 1. TEM images of (a) CN1 and (b) CN2, and the corresponding Raman spectra (c) and XRD pattern (d) of CN1.

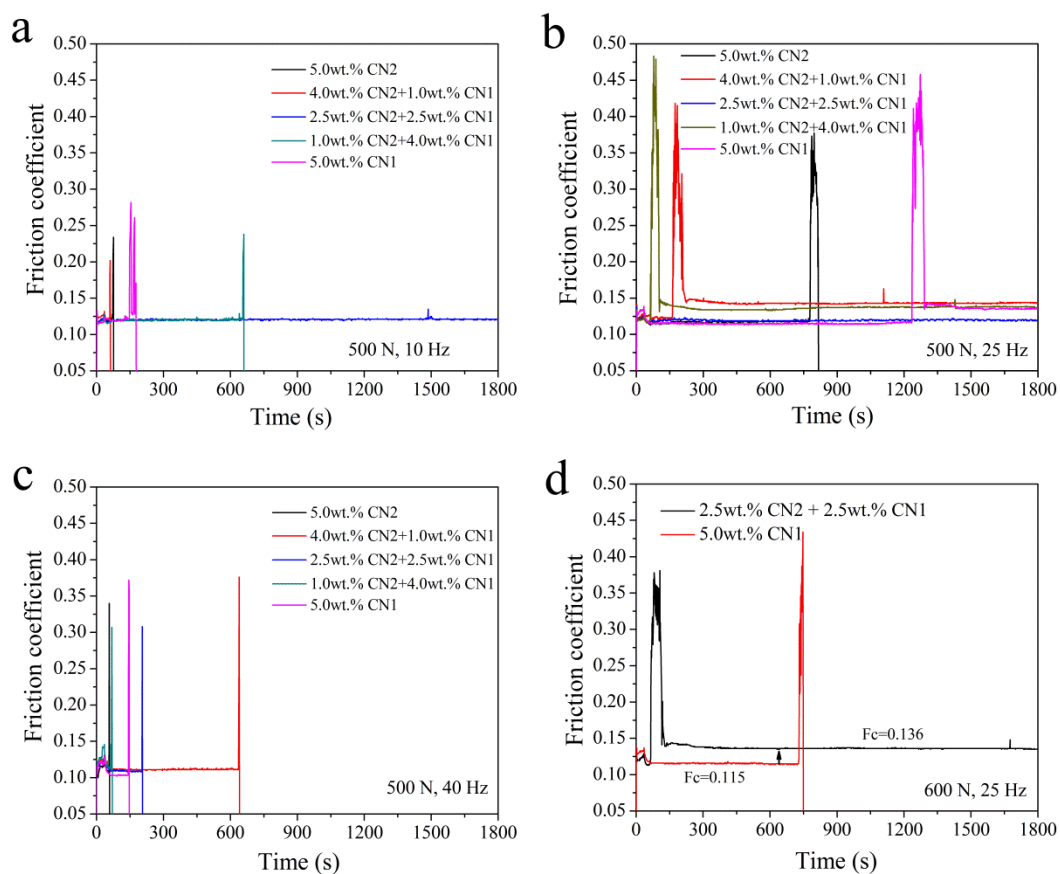


Figure 2. Friction coefficient of grease plus 5 wt.% CN additive with different CN1/CN2 mass ratio at (a) 500 N, 10 Hz; (b) 500 N, 25 Hz; (c) 500 N, 40 Hz; (d) 600 N, 25 Hz.

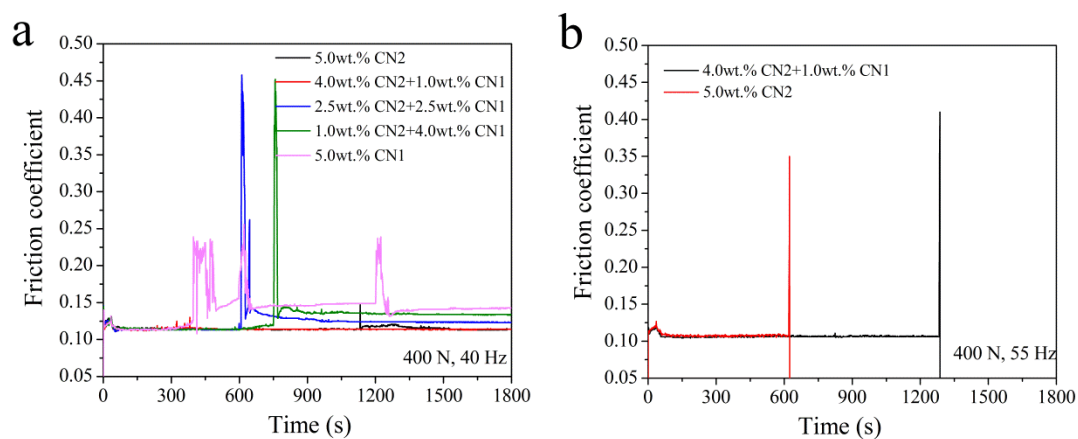


Figure 3. Friction coefficient of grease plus 5 wt.% CN additive with different CN1/CN2 mass ratio at (a) 400 N, 40 Hz; (b) 400 N, 55 Hz.

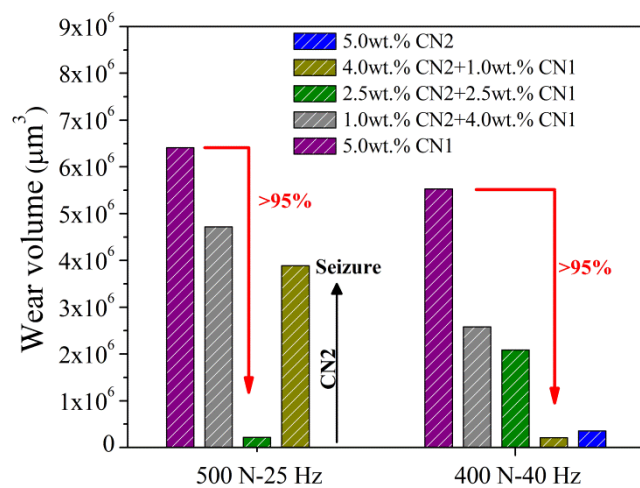


Figure 4. Wear volume of the lower disc lubricated by grease plus 5 wt.% CN additive with different CN1/CN2 mass ratio under rigorous condition (500 N, 25 Hz; 400 N, 40 Hz).

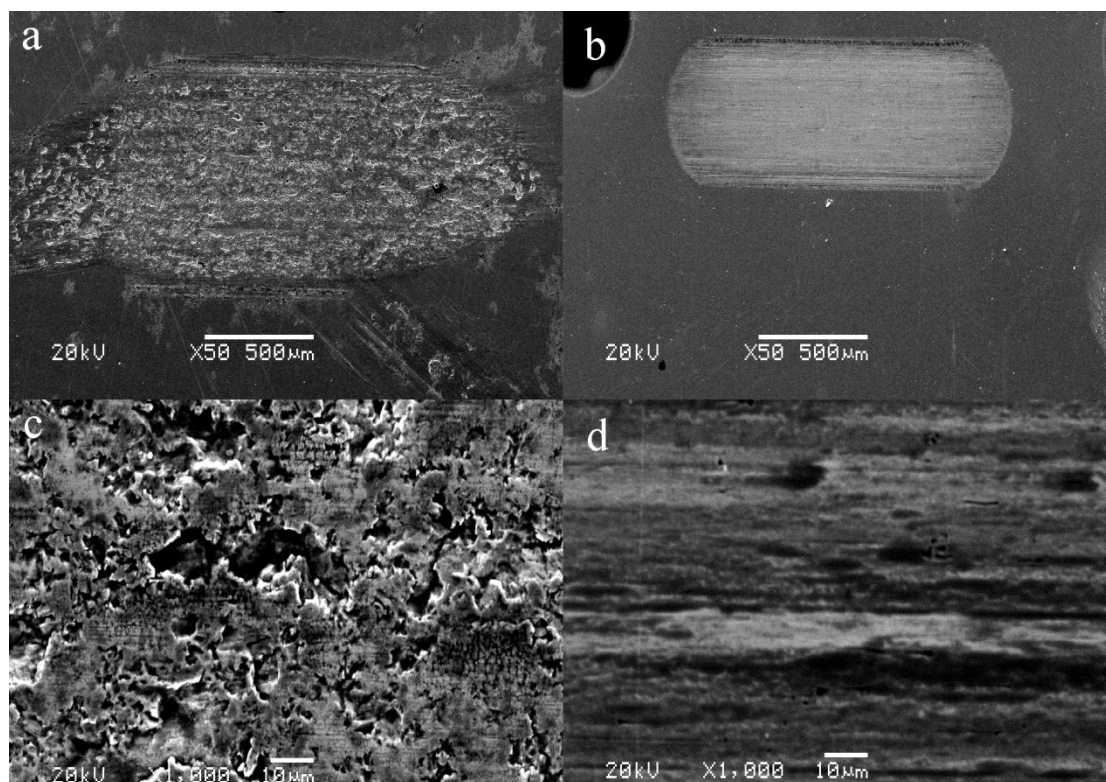


Figure 5. SEM images of wear scars lubricated by grease plus 5 wt.% CN additive with CN1/CN2 mass ratio of (a, c) 5:0 and (b, d) 1:4 under 400 N and 40 Hz.

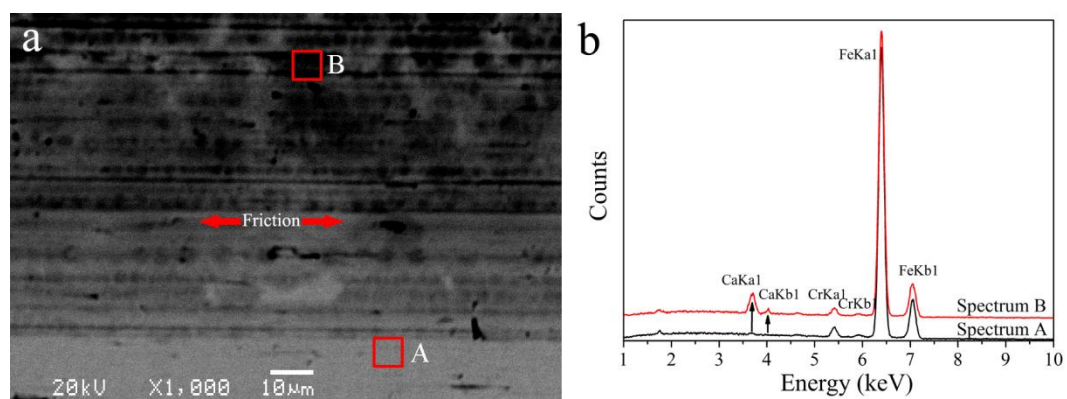


Figure 6. SEM/BSEI (a) and SEM/EDS (b) of wear scar lubricated by grease plus 5 wt.% CN additive with CN1/CN2 mass ratio of 1:4 under 400 N and 40 Hz.

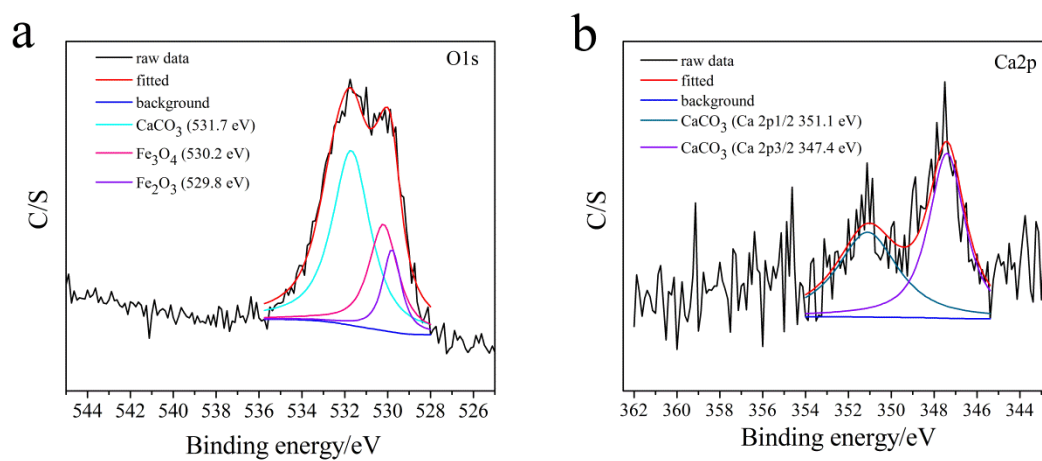


Figure 7. XPS spectra of wear scar lubricated by grease plus 5 wt.% CN additive with CN1/CN2 mass ratio of 1:4 under 400 N and 40 Hz.

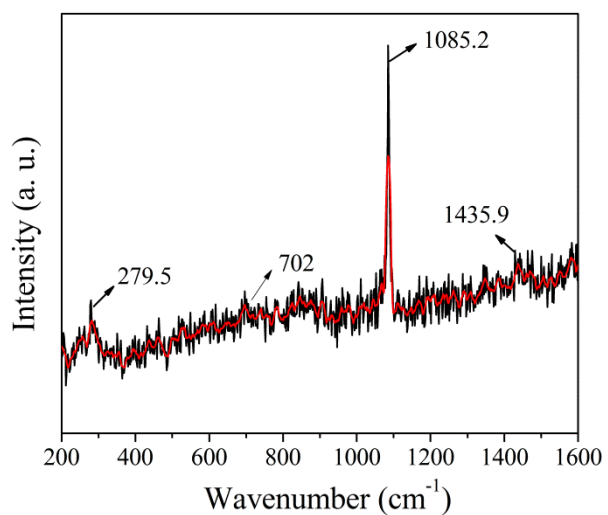


Figure 8. Raman spectra of wear scar lubricated by grease plus 5 wt.% CN additive with CN1/CN2 mass ratio of 1:4 under 400 N and 40 Hz.

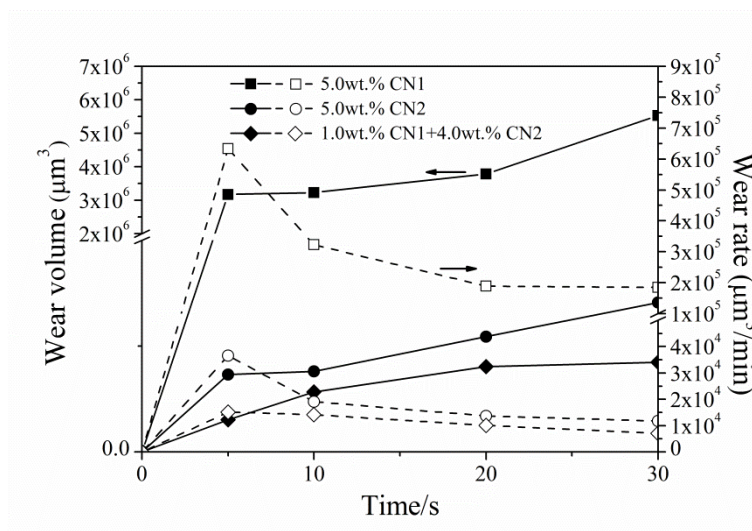
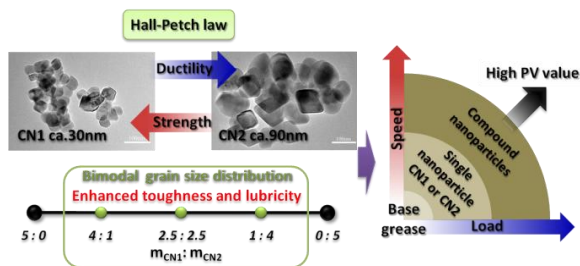


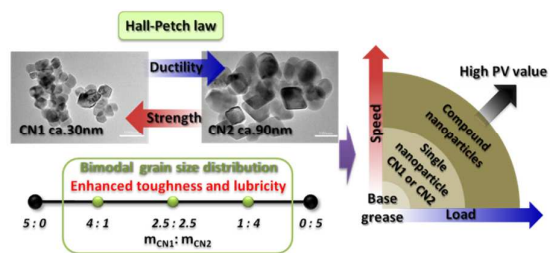
Figure 9. Wear volume and wear rate of wear scars lubricated by grease plus 5 wt.% CN additives under 400 N and 40 Hz with different CN1/CN2 mass ratio of (5:0; 1:4; 0:5).

Table of Contents



A novel reinforcing mechanism due to a bimodal grain size distribution in the tribological performance is reported.

Table of Contents



A novel reinforcing mechanism due to a bimodal grain size distribution in the tribological performance is reported.